Supporting Information for "No emergence of deep convection in the Arctic Ocean across CMIP6 models"

Céline Heuzé[1], and Hailong Liu[2]

[1]Department of Earth Sciences, University of Gothenburg, Gothenburg, Sweden

[2]School of Oceanography, Shanghai Jiao Tong University, Shanghai, China

Contents of this file

1. Text S1
2. Figures S1 to S2
3. Tables S1 to S4

Introduction

This document provides one supplementary text, two supplementary figures and four supplementary tables, referred to in the main text as Figures S1-s2 and Tables S1-S4, as well as the corresponding references.

Text S1. Choices of thresholds and robustness Globally, a deeper threshold than 500 m is commonly used to determine deep convection. Using a threshold of 1000 m instead of that of 500 m (chosen by consistency with Lique, Johnson, and Plancherel (2018)) does not significantly change the results. It only increased the number of models that are not convecting in the Arctic from 11 to 18, as can be seen on the main text Fig. 2. Time series of the yearly maximum mixed layer depth have been produced with the actual maximum regardless of time; April, month of deepest mixed layers for the few convecting models (not shown); and March, the month traditionally used and where the non-convecting models have their deepest mixed layers. The differences between the results were not significant. We therefore perform correlations and show results using the March mixed layers, for consistency with other studies.

The sensitivies and oceanic polar amplification values are not significantly affected by the choice of latitude bands. That is, the model order remains the same, only the individual models' magnitudes are changed. We chose to present the results that exclude 60°N to 75°N, as these are dominated by the biased Nordic Seas.

Finally, we tested different lags for the correlations and trends ranging from 1 to 6 months, as we aim to determine which process could be driving changes in the mixed layer depth. We show primarily those with one month lag (i.e. February salinity, temperature, sea ice and winds), that had the strongest signal-to-noise ratio. We also show as supplementary material the 6 months (September) values, although the reader must bear in mind that most models lose their September sea ice early (see supp. Fig. S1), therefore the statistics involving sea ice become less robust. We also tested different thresholds for

the ensemble and model agreement. Because of the low number of ensemble members for most models (especially so after removing the ones that have Arctic deep convection over 2015-2023), 66% was too restrictive: When rounded, it often meant "all ensemble members/models". Our choice of 50% threshold does not change the results significantly. In particular, it does not change the sign or relative magnitude of the correlations/trends. The trends are presented over exactly half of the run, but we tested with different number of years, with the entire run, and visually verified them for every model and ensemble member. We chose to present them separately over the two halves of the run as this matches the models' Arctic deep convection behaviour, as will be discussed.

References

Adcroft, A., Anderson, W., Balaji, V., Blanton, C., Bushuk, M., Dufour, C., ... Held et al., I. (2019). The GFDL global ocean and sea ice model OM4. 0: Model description and simulation features. *Journal of Advances in Modeling Earth Systems*, *11*, 3167-3211. doi: 10.1029/2019MS001726

Cao, J., Wang, B., Yang, Y.-M., Ma, L., Li, J., Sun, B., ... Wu, L. (2018). The NUIST Earth System Model (NESM) version 3: description and preliminary evaluation. *Geoscientific Model Development*, *11*. doi: 10.5194/gmd-11-2975-2018

Cherchi, A., Fogli, P., Lovato, T., Peano, D., Iovino, D., Gualdi, S., ... Navarra, A. (2019). Global mean climate and main patterns of variability in the CMCC-CM2 coupled model. *Journal of Advances in Modeling Earth Systems*, *11*, 185-209. doi: 10.1029/2018MS001369

Danabasoglu, G., Lamarque, J., Bacmeister, J., Bailey, D. A., DuVivier, A. K., Edwards,

J., & Emmons et al., L. K. (2020). The community earth system model version 2 (CESM2). *Journal of Advances in Modeling Earth Systems*, *12*. doi: 10.1029/2019MS001916

Dong, X., Jin, J., Liu, H., Zhang, H., Zhang, M., Lin, P., ... Lin, Z. (2021). CAS-ESM2.0 model datasets for the CMIP6 ocean model intercomparison project phase 1 (OMIP1). *Advances in Atmospheric Sciences*, *38*, 307-316. doi: 10.1007/s00376-020-0150-3

Döscher, R., Acosta, M., Alessandri, A., Anthoni, P., Arneth, A., Arsouze, T., ... Bernadello et al., R. (2021). The EC-Earth3 Earth System Model for the Climate Model Intercomparison Project 6. *Geosci. Model Dev. Discuss.*. doi: 10.5194/gmd-2020-446

Golaz, J., Caldwell, P., Van Roekel, L., Petersen, M., Tang, Q., Wolfe, J., ... Baldwin, S. (2019). The DOE E3SM coupled model version 1: Overview and evaluation at standard resolution. *Journal of Advances in Modeling Earth Systems*, *11*, 2089-2129. doi: 10.1029/2018MS001603

Hajima, T., Watanabe, M., Yamamoto, A., Tatebe, H., Noguchi, M. A., Abe, M., ... Kawamiya, M. (2020). Development of the MIROC-ES2L Earth system model and the evaluation of biogeochemical processes and feedbacks. *Geoscientific Model Development*, *13*. doi: 10.5194/gmd-13-2197-2020

He, B., Bao, Q., Wang, X., Zhou, L., Wu, X., Liu, Y., ... Li, J. (2019). CAS FGOALS-f3-L model datasets for CMIP6 historical atmospheric model intercomparison project simulation. *Advances in Atmospheric Sciences*, *36*, 771-778. doi: 10.1007/s00376

-019-9027-8

Kelley, M., Schmidt, G., Nazarenko, L., Bauer, S., Ruedy, R., Russell, G., ... Canuto, V. (2020). GISS-E2. 1: Configurations and climatology. *Journal of Advances in Modeling Earth Systems*, *12*, e2019MS002025. doi: 10.1029/2019MS002025

Kuhlbrodt, T., Jones, C., Sellar, A., Storkey, D., Blockley, E., Stringer, M., ... Calvert, D. (2018). The low-resolution version of HadGEM3 GC3. 1: Development and evaluation for global climate. *Journal of Advances in Modeling Earth Systems*, *10*. doi: 10.1029/2018MS001370

Li, L., Yu, Y., Tang, Y., Lin, P., Xie, J., Song, M., ... Pu, Y. (2020). The flexible global ocean-atmosphere-land system model grid-point version 3 (FGOALS-g3): description and evaluation. *Journal of Advances in Modeling Earth Systems*, *12*, e2019MS002012. doi: 10.1029/2019MS002012

Lique, C., Johnson, H., & Plancherel, Y. (2018). Emergence of deep convection in the Arctic Ocean under a warming climate. *Climate Dynamics*, *50*, 3833-3847. doi: 10.1007/s00382-017-3849-9

Lovato, T., Peano, D., ButenschÖn, M., Materia, S., Iovino, D., Scoccimarro, E., ... Masina, S. (2022). CMIP6 simulations with the CMCC Earth system model (CMCC-ESM2). *Journal of Advances in Modeling Earth Systems*, *14*, e2021MS002814. doi: 10.1029/2021MS002814

Mackallah, C., Chamberlain, M., Law, R., Dix, M., Ziehn, T., Bi, D., ... Evans, B. e. (2022). ACCESS datasets for CMIP6: methodology and idealised experiments. *Journal of Southern Hemisphere Earth Systems Science*, *72*, 93-116. doi:

10.1071/ES21031

Mauritsen, T., Bader, J., Becker, T., Behrens, J., Bittner, M., Brokopf, R., ... Fast, I. (2019). Developments in the MPI-M Earth System Model version 1.2 (MPI-ESM1. 2) and its response to increasing CO2. *Journal of Advances in Modeling Earth Systems*, *11*. doi: 10.1029/2018MS001400

Müller, W., Jungclaus, J., Mauritsen, T., Baehr, J., Bittner, M., Budich, R., ... Ilyina, T. (2018). A Higher-resolution Version of the Max Planck Institute Earth System Model (MPI-ESM1. 2-HR). *Journal of Advances in Modeling Earth Systems*, *10*. doi: 10.1029/2017MS001217

Rong, X. Y., Li, J., & Chen, H. M. (2019). Introduction of CAMS-CSM model and its participation in CMIP6. *Climate Change Res*, *6*. doi: 10.12006/j.issn.1673-1719 .2019.186

Séférian, R., Nabat, P., Michou, M., Saint-Martin, D., Voldoire, A., Colin, J., ... Sénési, S. (2019). Evaluation of CNRM Earth System Model, CNRM-ESM2-1: Role of Earth System Processes in Present-Day and Future Climate. *Journal of Advances in Modeling Earth Systems*. doi: 10.1029/2019MS001791

Seland, Ø., Bentsen, M., Olivié, D., Toniazzo, T., Gjermundsen, A., Graff, L., ... Schwinger, J. (2020). Overview of the Norwegian Earth System Model (NorESM2) and key climate response of CMIP6 DECK, historical, and scenario simulations. *Geoscientific Model Development*, *13*, 6165-6200. doi: 10.5194/gmd-13-6165-2020

Sellar, A., Jones, C., Mulcahy, J., Tang, Y., Yool, A., Wiltshire, A., ... Woodward, S. (2019). UKESM1: Description and evaluation of the UK Earth Sys-

tem Model. *Journal of Advances in Modeling Earth Systems*, *11*, 4513-4558. doi: 10.1029/2019MS001739

Semmler, T., Danilov, S., Gierz, P., Goessling, H., Hegewald, J., Hinrichs, C., ... Sein, D. (2020). Simulations for CMIP6 with the AWI climate model AWI-CM-1-1. *Journal of Advances in Modeling Earth Systems*, *12*, e2019MS002009. doi: 10.1029/2019MS002009

Sigmond, M., Anstey, J., Arora, V., Digby, R., Gillett, N., Kharin, V., ... Virgin, J. (2023). Improvements in the Canadian Earth System Model (CanESM) through systematic model analysis: CanESM5. 0 and CanESM5.1. *Geoscientific Model Development Discussions*, 1-54. doi: 10.5194/gmd-2023-52

Swart, N., Cole, J., Kharin, V., Lazare, M., Scinocca, J., Gillett, N., ... Jiao, Y. (2019). The Canadian Earth System Model version 5 (CanESM5. 0.3). *Geoscientific Model Development*, *12*. doi: 10.5194/gmd-2019-177

Tatebe, H., Ogura, T., Nitta, T., Komuro, Y., Ogochi, K., Takemura, T., ... Kimoto, M. (2019). Description and basic evaluation of simulated mean state, internal variability, and climate sensitivity in MIROC6. *Geoscientific Model Development*, *12*. doi: 10.5194/gmd-12-2727-2019

Voldoire, A., Saint-Martin, D., Sénési, S., Decharme, B., Alias, A., Chevallier, M., & Colin et al., J. (2019). Evaluation of CMIP6 DECK Experiments With CNRM-CM6-1. *Journal of Advances in Modeling Earth Systems*, *11*. doi: 10.1029/2019MS001683

Wu, T., Lu, Y., Fang, Y., Xin, X., Li, L., Li, W., ... Liu, X. (2019). The Beijing Climate Center Climate System Model (BCC-CSM): the main progress from CMIP5

to CMIP6. *Geoscientific Model Development*, *12*. doi: 10.5194/gmd-12-1573-2019

Yukimoto, S., Kawai, H., Koshiro, T., Oshima, N., Yoshida, K., Urakawa, S., ... Yabu, S. (2019). The Meteorological Research Institute Earth System Model version 2.0, MRI-ESM2. 0: Description and basic evaluation of the physical component. *Journal of the Meteorological Society of Japan*. doi: 10.2151/jmsj.2019-051

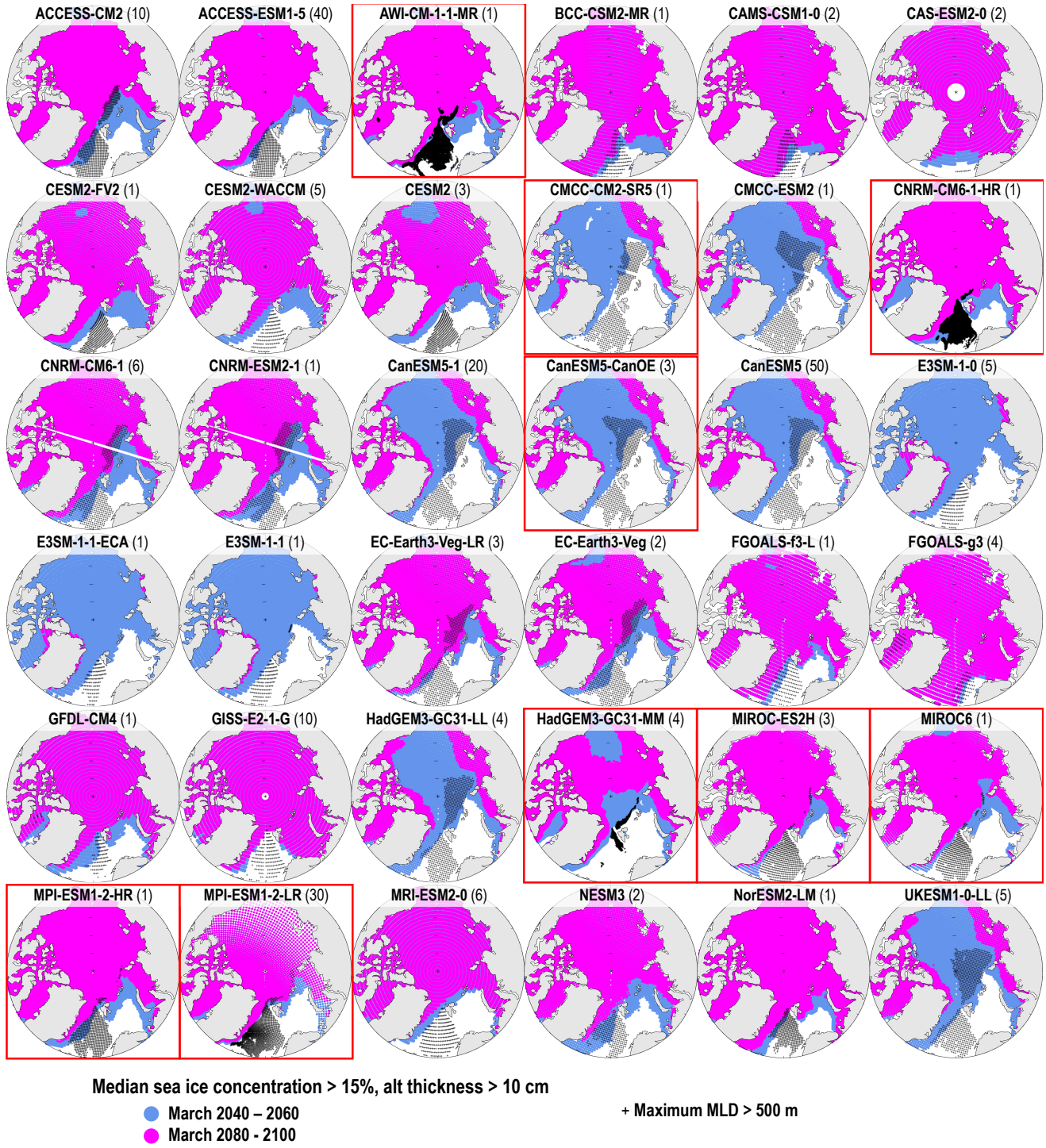

Figure S1. Median 2040-2060 (blue) and 2080-2100 (magenta overlaying the blue) March sea ice extent for all 36 models. Threshold is 15% sea ice concentration or 10 cm sea ice thickness. Black + indicate where the 2015-2100 maximum mixed layer depth (MLD) of Fig. 1 exceeds 500 m. Red boxes as per Fig. 1.

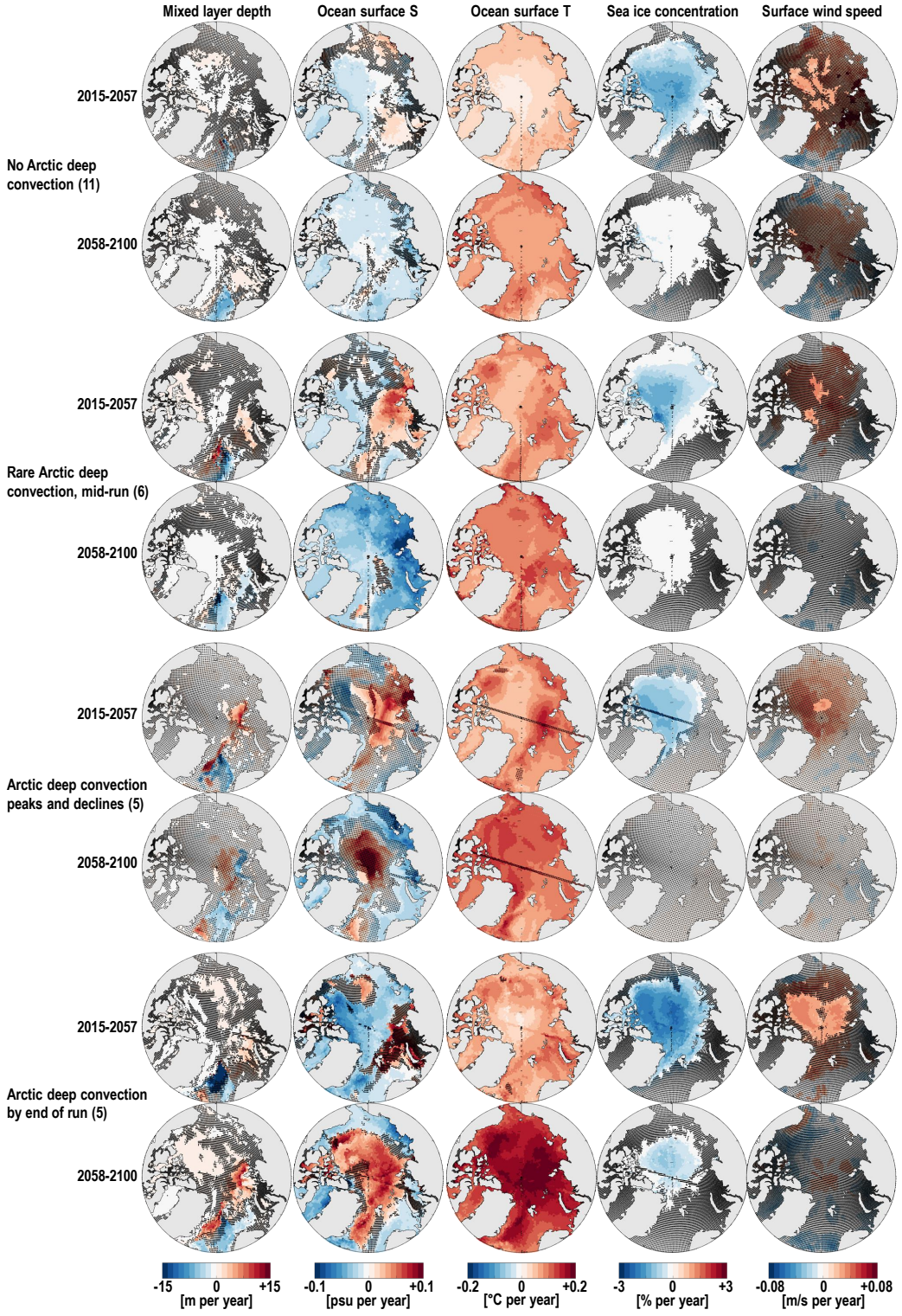

Figure S2. Composite trends based on the models' Arctic deep convection behaviours, for the first half of the 21st century run (top rows) and the second half (bottom rows), in March mixed layer depth (MLD, first column), and September ocean surface salinity, ocean surface temperature, sea ice concentration and surface wind speed. Behaviours are described to the left of the figure, and number of models for each behaviour is given in parentheses. For each panel, stippling indicates non-significant trends and/or model disagreement regarding the trend's sign.

Table S1. Models, ensemble members and corresponding grid type used in this study, along with the model's reference [a]

Model	Ensemble members	Grid	Reference
ACCESS-CM2	r1i1p1f1; r2i1p1f1; r3i1p1f1*; r4i1p1f1; r5i1p1f1; r6i1p1f1; r7i1p1f1; r8i1p1f1; r9i1p1f1*; r10i1p1f1*	gn	Mackallah et al. (2022)
ACCESS-ESM1-5	r1i1p1f1; r2i1p1f1; r3i1p1f1*; r4i1p1f1*; r5i1p1f1; r6i1p1f1; r7i1p1f1*; r8i1p1f1; r9i1p1f1; r10i1p1f1; r11i1p1f1*; r12i1p1f1; r13i1p1f1; r14i1p1f1; r15i1p1f1*;r16i1p1f1; r17i1p1f1; r18i1p1f1*; r19i1p1f1; r20i1p1f1; r21i1p1f1; r22i1p1f1*; r23i1p1f1*; r24i1p1f1; r25i1p1f1; r26i1p1f1; r27i1p1f1; r28i1p1f1; r29i1p1f1; r30i1p1f1; r31i1p1f1*; r32i1p1f1; r33i1p1f1; r34i1p1f1; r35i1p1f1; r36i1p1f1; r37i1p1f1; r38i1p1f1*; r39i1p1f1; r40i1p1f1	gn	Mackallah et al. (2022)
AWI-CM-1-1-MR*	r1i1p1f1*	gn	Semmler et al. (2020)
BCC-CSM2-MR	r1i1p1f1	gn	Wu et al. (2019)
CAMS-CSM1-0	r1i1p1f1; r2i1p1f1	gn	Rong, Li, and Chen (2019)
CAS-ESM2-0	r1i1p1f1; r3i1p1f1	gn	Dong et al. (2021)
CESM2-FV2	r1i2p2f1	gn	Danabasoglu et al. (2020)
CESM2-WACCM	r1i1p1f1; r2i1p1f1; r3i1p1f1; r4i1p1f1; r5i1p1f1	gr	Danabasoglu et al. (2020)
CESM2	r4i1p1f1; r10i1p1f1; r11i1p1f1	gn	Danabasoglu et al. (2020)
CMCC-CM2-SR5*	r1i1p1f1*	gn	Cherchi et al. (2019)
CMCC-ESM2	r1i1p1f1	gn	Lovato et al. (2022)
CNRM-CM6-1-HR*	r1i1p1f2*	gn	Voldoire et al. (2019)
CNRM-CM6-1	r1i1p1f2; r2i1p1f2; r3i1p1f2; r4i1p1f2; r5i1p1f2; r6i1p1f2	gn	Voldoire et al. (2019)
CNRM-ESM2-1	r1i1p1f2	gn	Séférian et al. (2019)
CanESM5-1	r1i1p1f1; r1i1p2f1; r2i1p1f1; r2i1p2f1; r3i1p1f1*; r3i1p2f1*; r4i1p1f1*; r4i1p2f1*; r5i1p1f1*; r5i1p2f1; r6i1p1f1*; r6i1p2f1*; r7i1p1f1; r7i1p2f1; r8i1p1f1*;r8i1p2f1; r9i1p1f1*; r9i1p2f1*; r10i1p1f1*; r10i1p2f1*	gn	Sigmond et al. (2023)
CanESM5-CanOE*	r1i1p2f1*; r2i1p2f1*; r3i1p2f1*	gn	Swart et al. (2019)

[a] Ensemble members marked with an asterisk (*) have deep convection in the Arctic over 2015 - 2023 already and were excluded from the correlation and trend analyses. Models marked with an asterisk (*) have deep convection in the Arctic over 2015 - 2023 already for all their ensemble members.

Table S2. Table S1 continued

Model	Ensemble members	Grid	Reference
CanESM5	r1i1p1f1*; r1i1p2f1*; r2i1p1f1*; r2i1p2f1*; r3i1p1f1*; r3i1p2f1*; r4i1p1f1*; r4i1p2f1; r5i1p1f1*; r5i1p2f1*; r6i1p1f1*; r6i1p2f1*; r7i1p1f1*; r7i1p2f1*; r8i1p1f1*;r8i1p2f1; r9i1p1f1*; r9i1p2f1*; r10i1p1f1*; r10i1p2f1*; r11i1p1f1*; r11i1p2f1*; r12i1p1f1*; r12i1p2f1*; r13i1p1f1*;r13i1p2f1*; r14i1p1f1*; r14i1p2f1; r15i1p1f1*; r15i1p2f1*; r16i1p1f1*; r16i1p2f1; r17i1p1f1*; r17i1p2f1; r18i1p1f1*; r18i1p2f1*; r19i1p1f1*; r19i1p2f1*; r20i1p1f1*; r20i1p2f1*; r21i1p1f1*; r21i1p2f1*; r22i1p1f1*; r22i1p2f1*; r23i1p1f1*; r23i1p2f1*; r24i1p1f1*; r24i1p2f1*; r25i1p1f1*; r25i1p2f1*	gn	Swart et al. (2019)
E3SM-1-0	r1i1p1f1; r2i1p1f1; r3i1p1f1; r4i1p1f1; r5i1p1f1	gr	Golaz et al. (2019)
E3SM-1-1-ECA	r1i1p1f1	gr	Golaz et al. (2019)
E3SM-1-1	r1i1p1f1	gr	Golaz et al. (2019)
EC-Earth3-Veg-LR	r1i1p1f1; r2i1p1f1; r3i1p1f1	gn	Döscher et al. (2021)
EC-Earth3-Veg	r1i1p1f1*; r2i1p1f1	gn	Döscher et al. (2021)
FGOALS-f3-L	r1i1p1f1	gn	He et al. (2019)
FGOALS-g3	r1i1p1f1; r2i1p1f1; r3i1p1f1; r4i1p1f1	gn	Li et al. (2020)
GFDL-CM4	r1i1p1f1	gr	Adcroft et al. (2019)
GISS-E2-1-G	r1i1p1f2; r1i1p3f1; r1i1p5f1*; r2i1p1f2; r2i1p3f1; r2i1p5f1; r3i1p1f2*; r3i1p3f1; r4i1p1f2; r4i1p3f1	gn	Kelley et al. (2020)
HadGEM3-GC31-LL	r1i1p1f3; r2i1p1f3; r3i1p1f3; r4i1p1f3	gn	Kuhlbrodt et al. (2018)
HadGEM3-GC31-MM*	r1i1p1f3*; r2i1p1f3*; r3i1p1f3*; r4i1p1f3*	gn	Kuhlbrodt et al. (2018)
MIROC-ES2H*	r1i1p4f2*; r2i1p4f2*; r3i1p4f2	gn	Hajima et al. (2020)
MIROC6*	r1i1p1f1*	gn	Tatebe et al. (2019)
MPI-ESM1-2-HR*	r2i1p1f1*	gn	Müller et al. (2018)
MPI-ESM1-2-LR*	r1i1p1f1*; r2i1p1f1*; r3i1p1f1*; r4i1p1f1*; r5i1p1f1*; r6i1p1f1*; r7i1p1f1*; r8i1p1f1*; r9i1p1f1*; r10i1p1f1*; r11i1p1f1*; r12i1p1f1*; r13i1p1f1*; r14i1p1f1*; r15i1p1f1*; r16i1p1f1*; r17i1p1f1*; r18i1p1f1*; r19i1p1f1*; r20i1p1f1*; r21i1p1f1*; r22i1p1f1*; r23i1p1f1*; r24i1p1f1*; r25i1p1f1*; r26i1p1f1*; r27i1p1f1*; r28i1p1f1*; r29i1p1f1*; r30i1p1f1*	gn	Mauritsen et al. (2019)
MRI-ESM2-0	r1i1p1f1; r1i2p1f1; r2i1p1f1; r3i1p1f1; r4i1p1f1; r5i1p1f1*	gr	Yukimoto et al. (2019)
NESM3	r1i1p1f1; r2i1p1f1	gn	Cao et al. (2018)
NorESM2-LM	r1i1p1f1	gn	Seland et al. (2020)
UKESM1-0-LL	r1i1p1f2; r2i1p1f2*; r3i1p1f2; r4i1p1f2; r8i1p1f2*	gn	Sellar et al. (2019)

Table S3. Table version of Figure 2: Models; number of ensemble members used[a]; across-ensemble minimum - median - maximum of the yearly maximum mixed layer depth (in meters); across-ensemble minimum - mode - maximum number of years with deep convection in the Arctic; type of Arctic deep convection behaviour (for the composites)[b]

Model	Nb. members	Across-ensemble max MLD min - median - max	Across-ensemble years min - mode - max	Type
ACCESS-CM2	7	883 - 1041 - 1134	10 - 23 - 25	Late
ACCESS-ESM1-5	30	661 - 1019 - 1356	2 - 4 - 17	MidR
BCC-CSM2-MR	1	104	0	NoDC
CAMS-CSM1-0	2	198 - 224 - 251	0 - 0 - 0	NoDC
CAS-ESM2-0	2	157 - 165 - 173	0 - 0 - 0	NoDC
CESM2-FV2	1	97	0	NoDC
CESM2-WACCM	5	99 - 101 - 102	0 - 0 - 0	NoDC
CESM2	3	108 - 108 - 111	0 - 0 - 0	NoDC
CMCC-ESM2	1	1147	73	MidD
CNRM-CM6-1	6	894 - 946 - 1045	22 - 22 - 33	Late
CNRM-ESM2-1	1	901	21	Late
CanESM5-1	8	1011 - 1193 - 1808	43 - 65 - 69	MidD
CanESM5	6	1262 - 1497 - 1969	49 - 55 - 60	MidD
E3SM-1-0	5	492 - 575 - 698	0 - 1 - 4	MidR
E3SM-1-1-ECA	1	497	0	NoDC
E3SM-1-1	1	701	4	MidR
EC-Earth3-Veg-LR	3	1207 - 1439 - 1450	16 - 16 - 31	Late
EC-Earth3-Veg	1	1322	33	Late
FGOALS-f3-L	1	350	0	NoDC
FGOALS-g3	4	229 - 255 - 258	0 - 0 - 0	NoDC
GFDL-CM4	1	166	0	NoDC
GISS-E2-1-G	8	302 - 625 - 875	0 - 0 - 10	MidR
HadGEM3-GC31-LL	4	1325 - 1418 - 2552	47 - 47 - 72	MidD
MRI-ESM2-0	5	352 - 511 - 554	0 - 0 - 2	MidR
NESM3	2	295 - 437 - 579	0 - 0 - 1	MidR
NorESM2-LM	1	92	0	NoDC
UKESM1-0-LL	3	1097 - 1325 - 1517	47 - 47 - 56	MidD

[a] The ensemble members are those listed in supp. Tables S1 and S2 without an asterisk, i.e. that do not have deep convection in the Arctic already over 2015-2023.

[b] Types are: "NoDC", no deep convection in the Arctic over 2015 - 2100 in SSP5-8.5; "MidR", rare Arctic deep convection, mid-run; "MidD", Arctic deep convection peaks mid-run and declines; "Late", Arctic deep convection late in the run.

Table S4. Correlation coefficient[a] for each model between the February ocean surface salinity (S), temperature (T), sea ice concentration (SIC) and surface wind speed (Wind), for the Eurasian basin (EB) and, for the models with Arctic deep convection, where the maximum MLD of Fig. 1 exceeds 500 m (DC). Bold fonts highlight the maximum correlation for each model.

Model	Region	S vs T	S vs SIC	S vs Wind	T vs SIC	T vs Wind	SIC vs Wind
BCC-CSM2-MR	EB	**-0.84**	0.26	0.25	-0.42	-0.23	-0.24
CAMS-CSM1-0	EB	**-0.98**	-0.26	0.24	-0.24	0.26	-0.39
CAS-ESM2-0	EB	-0.76	0.86	-0.34	**-0.78**	0.29	-0.32
CESM2-FV2	EB	**-0.98**	0.55	-0.40	-0.69	0.39	-0.36
CESM2-WACCM	EB	-0.78	0.60	-0.33	**-0.89**	0.36	-0.36
CESM2	EB	-0.77	0.76	-0.45	**-0.86**	0.37	-0.46
E3SM-1-1-ECA	EB	0.57	-0.41	0.35	**-0.75**	0.48	-0.58
FGOALS-f3-L	EB	0.23	0.25	0.27	**-0.66**	0.29	-0.29
FGOALS-g3	EB	-0.27	**0.54**	0.28	-0.32	-0.26	-0.24
GFDL-CM4	EB	**-0.90**	0.46	-0.29	-0.58	0.35	-0.31
NorESM2-LM	EB	**-0.89**	0.30	0.27	-0.41	0.27	-0.39
ACCESS-ESM1-5	EB	-	-	-	-	-	-
	DC	-	-	-	-	-	-
E3SM-1-0	EB	-0.25	0.27	0.25	**-0.80**	0.43	-0.55
	DC	-	-	-	-	-	-
E3SM-1-1	EB	-0.48	0.40	-0.22	**-0.84**	0.44	-0.54
	DC	-	-0.27	0.42	**-0.86**	0.56	-0.60
GISS-E2-1-G	EB	**-0.99**	0.64	0.24	-0.65	0.23	-0.30
	DC	0.72	-0.52	0.49	**-0.75**	0.48	-0.44
MRI-ESM2-0	EB	-0.70	0.61	-0.25	**-0.90**	0.31	-0.32
	DC	-	-	-	-	-	-
NESM3	EB	0.43	-0.48	0.32	**-0.84**	0.30	-0.35
	DC	-	-	-	-	-	-
CMCC-ESM2	EB	0.64	-0.62	0.40	**-0.80**	0.47	-0.58
	DC	0.70	-0.66	0.41	**-0.76**	0.47	-0.57
CanESM5-1	EB	0.32	-0.40	0.39	**-0.84**	0.54	-0.63
	DC	0.34	-0.42	0.39	**-0.83**	0.57	-0.67
CanESM5	EB	-	-	-	-	-	-
	DC	-	-	-	-	-	-
HadGEM3-GC31-LL	EB	-	-	-	-	-	-
	DC	-	-	-	-	-	-
UKESM1-0-LL	EB	0.70	-0.74	0.48	**-0.84**	0.52	-0.58
	DC	0.72	-0.75	0.50	**-0.84**	0.55	-0.61
ACCESS-CM2	EB	-0.31	-0.35	-0.23	**-0.83**	0.40	-0.44
	DC	0.55	-0.53	0.30	**-0.82**	0.41	-0.45
CNRM-CM6-1	EB	0.28	-0.30	0.31	**-0.82**	0.40	-0.50
	DC	0.39	-0.40	0.33	**-0.86**	0.50	-0.59
CNRM-ESM2-1	EB	0.38	-0.39	0.34	**-0.79**	0.50	-0.54
	DC	0.44	-0.44	0.37	**-0.84**	0.54	-0.57
EC-Earth3-Veg-LR	EB	0.41	-0.54	0.33	**-0.77**	0.43	-0.45
	DC	0.49	-0.62	0.41	**-0.81**	0.44	-0.50
EC-Earth3-Veg	EB	0.41	-0.44	0.32	**-0.76**	0.34	-0.37
	DC	0.56	-0.54	0.34	**-0.77**	0.40	-0.48

[a] Only correlations significant at 95% are shown; for models with more than one ensemble member, median of the correlations of the dominating sign.